

THE EFFECTS OF ALFVÉN WAVES AND RADIATION PRESSURE IN DUSTY WINDS OF LATE-TYPE STARS II: DUST-CYCLOTRON DAMPING

A. A. Vidotto and V. Jatenco-Pereira¹

*Instituto de Astronomia, Geofísica e Ciências Atmosféricas, Universidade de São Paulo,
Rua do Matão 1226, 05508-900 São Paulo, SP, Brazil*

ABSTRACT

There are in the literature several theories to explain the mass loss in stellar winds. In particular, for late-type stars, some authors have proposed a wind model driven by an outward-directed flux of damped Alfvén waves. The winds of these stars present great amounts of dust particles that, if charged, can give rise to new wave modes or modify the pre-existing ones. In this work, we study how the dust can affect the propagation of Alfvén waves in these winds taking into account a specific damping mechanism, dust-cyclotron damping. This damping affects the Alfvén wave propagation near the dust-cyclotron frequency. Hence, if we assume a dust size distribution, the damping occurs over a broad band of wave frequencies. In this work, we present a model of Alfvén wave-driven winds using the dust-cyclotron damping mechanism. On the basis of coronal holes in the Sun, which present a superradial expansion, our model also assumes a diverging geometry for the magnetic field. Thus, the mass, momentum, and energy equations are obtained and then solved in a self-consistent approach. Our results of wind velocity and temperature profiles for a typical K5 supergiant star shows compatibility with observations. We also show that, considering the presence of charged dust particles, the wave flux is less damped due to the dust-cyclotron damping than it would be if we consider some other damping mechanisms studied in the literature, such as nonlinear damping, resonant surface damping, and turbulent damping.

Subject headings: MHD — plasmas — stars: winds, outflows — stars: late-type — supergiants — dust, extinction

1. INTRODUCTION

Cool supergiant stars present high mass loss rates, $\dot{M} \sim 10^{-8} - 10^{-5} M_{\odot} \text{ yr}^{-1}$, and low terminal velocities, $u_{\infty} \sim 10 - 100 \text{ km s}^{-1}$ (Cassinelli 1979), which are less than the escape velocity at the stellar surface (v_{e0}). Typically, it is observed that $u_{\infty} \lesssim v_{e0}/2$. Although the physical mechanism that drives these winds is still poorly known, driving the wind with magnetohydrodynamic waves is one of the most promising mechanism proposed to date. Several authors (e.g., Liberatore et al. 2001; Elitzur & Ivezić 2001; Höfner et al. 2003; Woitke & Niccolini 2005), motivated by the observed high stellar luminosity and low effective temperature of these stars, have proposed radiatively dust driven wind models to explain the wind acceleration. Acoustic waves generated at a pulsating phase could provide a propitious ambient medium for dust formation; this is, a high-density region with low temperature. Hence, radiative pressure acting on dust particles could accelerate the grain and, if the gas and the dust were dynamically coupled, grains could drag the gas and provide the mass loss. However, this mechanism fails when gas and dust are not well coupled (Sandin & Höfner 2003). Another failing aspect of this mechanism is that there are observations attesting that the wind forms before the grain formation point (Carpenter et al. 1995).

In this aspect, Alfvén waves might play an important role in these scenarios, producing significant mass loss and low terminal velocities (Lamers & Cassinelli 1999, p. 294). In this mechanism, the wave magnetic pressure gradient is added into the momentum equation in order to drive the wind.

Hartmann & MacGregor (1980) investigated the effects of Alfvén waves on the outer atmospheres of cool supergiant stars. They estimated an initial wave flux of $\sim 10^6 \text{ ergs cm}^{-2} \text{ s}^{-1}$. This flux is of the same order of magnitude as the one estimated for the solar wind (Banerjee et al. 1998). However, they found that undamped waves led to very high terminal wind velocities. In order to obtain terminal velocities that were in reasonable agreement with observations of cool supergiant stars, it was necessary to dissipate the waves on a length scale of $\sim r_0$ (r_0 is the star radius). The physical mechanism responsible for the damping was left unspecified. Holzer et al. (1983) argued that this length scale was very restrictive and that we could not observe a large variety of stars if we had such selective dissipation scale for the waves. This problem was known as the *fine tuning problem*. Jatenco-Pereira & Opher (1989) showed that flux tubes expanding superradially from the stellar surface, as is observed to happen in solar coronal holes (Cranmer & van Ballegoijen 2005), could account for a broad band of dissipation scales, overcoming this problem.

In Falceta-Gonçalves & Jatenco-Pereira (2002, hereafter Paper I), a hybrid model was presented, in which the effects of a flux of Alfvén waves acting together with radiation pressure on grains were analyzed as acceleration mechanisms of winds of cool supergiant stars.

In that model, an empirical temperature profile was introduced. The presence of grains had two roles in that model: grains were used to simulate a strong damping mechanism for the waves and as an additional acceleration mechanism due to the exertion of radiation pressure on them. Hence, a more realistic wind model showing results consistent with observations was obtained.

Here, we present a model in which a flux of Alfvén waves propagating outward from the star is damped due to the interaction between the waves and charged dust particles, thus, accelerating the wind. In order to obtain both the temperature and the velocity profiles, we solve the mass, the momentum, and the energy equations of the wind. In this work, we improve the model presented in Paper I by: (1) inserting the energy equation into the model in order to obtain the temperature profile of the wind; and (2) inserting a more realistic damping mechanism for the waves due to the presence of grains. Here, we examine the influence of this damping mechanism instead of simulating a strong damping. In §2, we describe the model used to accelerate the wind: we describe the modified wave dispersion relation due to the presence of charged dust in §2.1, the geometry considered for the magnetic field lines in §2.2, the equations that describe the wind dynamics in §2.3, and the radiation pressure on dust in §2.4. In §3 and §4, we present our results and conclusions.

2. MODEL

2.1. Dust-Cyclotron Damping

The propagation and damping of Alfvén waves in a dusty plasma has been considered by many authors (Phillip et al. 1987; Mendis & Rosenberg 1992; Shukla 1992; Falceta-Gonçalves et al. 2003). Dust grains immersed in an ambient plasma become charged due to plasma ion and electron fluxes into grain surfaces. Although the number of dust particles is smaller than the number of ions, the process of dust charging is efficient and these particles can obtain charges $q_d = -z_d e$ for z_d on the order of $\sim 10^0 - 10^3$ in astrophysical media (Goertz 1989; Mendis & Rosenberg 1994). Once charged, these particles suffer the influence of the magnetic field which gives rise to a cyclotron frequency. Thus, they can modify the plasma behavior in different ways. In particular, charged dust particles introduce a cutoff (resonance) in the Alfvén wave spectrum at the dust cyclotron frequency. For the ions, this resonance occurs in a narrow range of higher frequencies, which are unimportant in the systems under consideration. On the other hand, the dust cyclotron resonance occurs at low frequencies and it can be an important damping mechanism for the waves.

If a distribution of grain sizes is considered, then we obtain a band of resonance fre-

quencies from the minimum dust-cyclotron frequency ω_{\min} to the maximum dust-cyclotron frequency ω_{\max} . According to Mathis et al. (1977), we can describe the distribution of grain sizes in the interstellar medium by a power law (MRN distribution):

$$f(\mathcal{R}) d\mathcal{R} = c_p \mathcal{R}^{-p} d\mathcal{R}, \quad (1)$$

where $c_p = (p-1)/(1-a_m^{1-p})$, $\mathcal{R} = a/a_{\min}$ is a dimensionless radius, a is the grain radius, $a_m = a_{\max}/a_{\min}$, and a_{\min} and a_{\max} are the minimum and the maximum dust radii, respectively. Observationally, the parameter p depends on the dust constituent and on the environment. In this work we consider $p = 4$, as used by Cramer et al. (2002). In this case, we have $c_4 = 3/(1-a_m^{-3})$.

The wave propagation in dusty plasma is modified and some new and interesting effects take place (Wardle & Ng 1999; Cramer 2001). The dispersion relation of the Alfvén waves, with frequencies smaller than the ion cyclotron frequency, considering dust particles with constant charges in a neutral and cold dusty plasma, is given by (Cramer et al. 2002)

$$k_z^2 = u_1 \pm u_2, \quad (2)$$

where:

$$u_1 = \frac{\omega^2 \Omega_i^2}{v_{Ai}^2 (\Omega_i^2 - \omega^2)} + \frac{\omega^2 \Omega_{d0}^2}{s v_{Ad}^2} \int_1^{a_m} \frac{f(\mathcal{R}) d\mathcal{R}}{\mathcal{R} (\Omega_{d0}^2 / \mathcal{R}^4 - \omega^2)}, \quad (3)$$

and

$$u_2 = \frac{\omega^3 \Omega_i}{v_{Ai}^2 (\Omega_i^2 - \omega^2)} + \frac{\omega^3 \Omega_{d0}}{s v_{Ad}^2} \int_1^{a_m} \frac{\mathcal{R} f(\mathcal{R}) d\mathcal{R}}{\Omega_{d0}^2 / \mathcal{R}^4 - \omega^2}. \quad (4)$$

Here $s = c_4 \ln(a_m)$, ω is the angular wave frequency, Ω_i is the ion cyclotron frequency, $\Omega_{d0} = q_{\min} B / (m_{\min} c) \equiv \omega_{\max}$ is the maximum dust cyclotron frequency (i.e., for the minimum dust grain with mass m_{\min} and charge q_{\min}), and $v_{A\alpha} = B / (\sqrt{4\pi\rho_\alpha})$ is the Alfvén speed of the α species. Here $\alpha = i$ and d for ions and dust, respectively, B is the magnetic field intensity, ρ_α is the α species density, and c is the speed of light. In order to calculate the grain mass, we assume spherical silicates grains with $\rho_{\text{sil}} = 3.3 \text{ g cm}^{-3}$.

Dust grains are usually negatively charged, with many electrons collected on each particulate. The mean grain particle charge can be obtained for each dust radius by considering the charge current equilibrium over the dust surface. The equilibrium equation, if we consider a Maxwellian distribution of velocities, is given by (Vladimirov 1997)

$$\frac{\omega_{pi}^2}{\omega_{pe}^2} \left(1 + \frac{z_d e^2}{a k_B T} \right) = \frac{v_{Ti}}{v_{Te}} \exp \left\{ -\frac{z_d e^2}{a k_B T} \right\}. \quad (5)$$

The plasma frequency, $\omega_{p\beta}$, for electrons ($\beta = e$) or ions ($\beta = i$) is given by:

$$\omega_{p\beta} = \sqrt{\frac{4\pi\rho_\beta q_\beta^2}{m_\beta^2}} \quad (6)$$

and the thermal velocity, $v_{T\beta}$, is given by:

$$v_{T\beta} = \sqrt{\frac{k_B T}{m_\beta}}, \quad (7)$$

where k_B is the Boltzmann constant.

The left-hand polarized wave (minus sign in eq. [2]) interacts with ions and is not affected by the negatively charged dust particles resonance. The right-hand polarized wave (plus sign in eq. [2]) is the mode damped by the dust resonance. In the case of $\omega_{\min} < \omega < \omega_{\max}$, the integral over the particle's radius has singularities, whose residues give the complex part of the wave number ($k_z \equiv k_{\mathcal{R}} + ik_{\mathcal{C}}$) and that leads to the dust-cyclotron damping of the waves, with damping length:

$$L(\omega) = \frac{2\pi}{k_{\mathcal{C}}(\omega)}. \quad (8)$$

We adopt a particle radius distribution from $a_{\min} = 5.0 \times 10^{-7}$ cm to $a_{\max} = 2.5 \times 10^{-5}$ cm (Rogers & Glassgold 1991). In order to calculate ρ_d , we adopt a gas-to-dust ratio given by:

$$R_{gd} = \frac{\rho}{\rho_d}, \quad (9)$$

where ρ is the gas density.

In this work, we do not develop a self-consistent model for the grain nucleation. According to the model of Dominik et al. (1989) for dust-driven winds around carbonated stars, near the critical point ($\sim 1.5 r_0$) there is an intense grain formation. For $r < 1.5 r_0$, grains are only formed locally, and beyond $2.0 r_0$, dust is already condensed into an envelope around the star. On the basis of this scenario, we adopt the following situation. For $r \gtrsim 2.0 r_0$, $R_{gd} \simeq 200$ (Knapp 1985; Heras & Hony 2005), which implies that the dust envelope has already been formed. Near the wind base, $R_{gd} \gg 200$, which implies the existence of a negligible dust quantity. Between the wind base and $\sim 2.0 r_0$, R_{gd} decreases exponentially, which indicates that the grains are being formed until R_{gd} reaches its minimum value of $\simeq 200$.

2.2. Magnetic Field Geometry

It is beyond the scope of this paper to discuss magnetic field generation in late-type stars. However, many works studying field generation have been presented in the literature (Blackman et al. 2001; Soker & Zoabi 2002; Dorch 2004). These works are motivated by observations of, for instance, maser polarization (Vlemmings et al. 2002) or X-ray emission

(Ayres et al. 2003) from late-type stars, which are taken as an indicative of the presence of magnetic fields around them. Hence, jointly with perturbations (e.g., convective motions), the basic ingredient for Alfvén wave generation is present in the atmospheres of late-type stars.

On the basis of this assumption, Jatenco-Pereira & Opher (1989) suggested a model for mass loss in late-type stars driven by an outward flux of damped Alfvén waves that took into account our knowledge of coronal holes in the Sun. It is known that the coronal holes are the source of the high-speed solar wind streams at the Earth’s orbit (e.g., Peter & Judge 1999). The role of Alfvén waves in accelerating the fast solar wind and the heating of plasma in the open magnetic structures of the solar corona has been discussed since the pioneering work of Parker (1965) (e.g., Rosenthal et. al 2002; Suzuki & Inutsuka 2005, among others). The area expansion of a solar coronal hole is 5 – 13 times greater than that for a radial expansion (Lie-Svendson et al. 2002; Esser et al. 2005; Tu et al. 2005). For simplicity, we assume that in the wind of a typical K5 supergiant star, the non-radial expansion factor is

$$F = \frac{\Omega}{\Omega_0} = 10, \quad (10)$$

where Ω_0 and Ω are the solid angles at the stellar surface and at the edge of the coronal hole, respectively. Hence, in order to reproduce the coronal holes, we use a diverging geometry suggested by Kuin & Hearn (1982) for the magnetic field. The cross section of a flux tube at a radial distance r is given by

$$A(r) = \begin{cases} A(r_0)(r/r_0)^S & \text{if } r \leq r_t \\ A(r_0)(r_t/r_0)^S(r/r_t)^2 & \text{if } r > r_t, \end{cases}$$

where S is a parameter that determines the divergence of the geometry up to the transition radius r_t , as shown in Figure 1. For a given S , r_t is easily obtained:

$$F = \frac{\Omega}{\Omega_0} = \frac{A(r_t)/r_t^2}{A(r_0)/r_0^2} = \left(\frac{r_t}{r_0}\right)^{S-2}. \quad (11)$$

Hence, we have

$$r_t = F^{1/(S-2)} r_0. \quad (12)$$

Then, when we consider this geometry, conservation of magnetic flux yields a magnetic field intensity $B(r) \propto A(r)^{-1}$.

2.3. The Wind Equations

The mass, momentum, and energy equations are the equations responsible in driving the wind:

The mass equation It expresses the continuity of matter. For a flow velocity u , we have:

$$\rho u A(r) = \mathcal{C}. \quad (13)$$

The constant \mathcal{C} in equation (13) is computed at the stellar surface: $\mathcal{C} = \rho_0 u_0 A(r_0)$, where the subscript “0” indicates that the parameter is being evaluated at $r = r_0$.

The momentum equation In this model, we assume that the forces acting on the wind particles are the gravitational force, the gas pressure gradient, and the wave magnetic pressure gradient. Hence, if we assume a steady flow, the equation of motion can then be written as:

$$\rho u \frac{du}{dr} = -\rho \frac{GM_\star}{r^2} - \frac{dP}{dr} - \frac{1}{2} \frac{d\epsilon}{dr}, \quad (14)$$

where $P = \rho k_B T / m$ is the gas pressure, m is the average mass per particle, ϵ is the energy density of the Alfvén waves, and GM_\star / r^2 is the gravitational acceleration. The last term in equation (14) is the wave magnetic pressure gradient. As dP/dr and $d\epsilon/dr$ are both negative quantities, we can see that the gas and the wave pressure gradients act in the opposite direction to the gravitational attraction.

The energy equation In order to compute the temperature profile of the wind, one needs to evaluate the energy equation. In the present model, the wind temperature is determined through the balance between wave heating, adiabatic expansion, and radiative cooling. If we neglect conduction and assume a perfect gas, we write the energy equation as (Hartmann et al. 1982)

$$\rho u \frac{d}{dr} \left(\frac{u^2}{2} + \frac{5 k_B T}{2 m} - \frac{v_e^2}{2} \right) + \frac{u}{2} \frac{d\epsilon}{dr} = (Q - P_R), \quad (15)$$

where v_e is the escape velocity. The term $(u/2)d\epsilon/dr$ is the rate at which the waves do work on the gas. The quantity Q is the wave heating rate, i.e., the rate at which the gas is being heated due to the dissipation of wave energy, and P_R is the radiative cooling rate, both in units of $\text{ergs cm}^{-3} \text{ s}^{-1}$.

The radiative cooling rate is given by:

$$P_R = \Lambda n_e n_H, \quad (16)$$

where n_e is the electron density, n_H is the hydrogen density, and Λ is the radiative loss function. Here, we adopt the value of Λ given by Schmutzler & Tscharnuter (1993) and calculate n_e as did Hartmann & MacGregor (1980).

In order to evaluate the wave heating rate Q , one needs to know how the wave energy is being dissipated. In our model, we assume that Alfvén waves are damped by the dust-cyclotron damping mechanism, which has a damping length $L(\omega)$ given by equation (8). It is important to note that each wave frequency is damped by a different amount (see §3 for a discussion). Hence, the wave heating rate must be different for each wave frequency. The wave heating rate that enters equation (15) is, then, calculated as follows:

$$Q = \int_{\omega_{\min}}^{\omega_{\max}} Q(\omega) d\omega, \quad (17)$$

where $Q(\omega)$ is the wave heating rate per frequency and it is directly related to the wave energy density per unit frequency $\epsilon(\omega)$ and the damping length $L(\omega)$ associated with it. Hence, we have (Hollweg 1973)

$$Q(\omega) = \frac{\epsilon(\omega)}{L(\omega)}(u + v_A). \quad (18)$$

Similarly, the wave energy density ϵ needs to be calculated over the frequency band. Hence, we have:

$$\epsilon = \int_{\omega_{\min}}^{\omega_{\max}} \epsilon(\omega) d\omega \quad (19)$$

and, for each frequency, it is calculated as (Jatenco-Pereira & Opher 1989):

$$\epsilon(\omega) = \epsilon_0(\omega) \frac{M_0}{M} \left(\frac{1 + M_0}{1 + M} \right)^2 \exp \int_{r_0}^r -\frac{1}{L(\omega)} dr', \quad (20)$$

where $M = u/v_A$ is the Alfvén Mach number with $v_A = (B/\sqrt{4\pi\rho})$.

Tu et al. (1989) observed an Alfvén wave spectrum propagating in the solar wind and inferred for the low-frequency range that $\epsilon(\omega) \propto \omega^{-\beta}$, with $\beta \sim 0.6$. Here, we assume that the initial energy density of Alfvén waves propagating in the winds of cool supergiant stars behaves similarly:

$$\epsilon_0(\omega) = \epsilon_0(\omega_0) \left(\frac{\omega}{\omega_0} \right)^{-\beta}, \quad (21)$$

where $\epsilon_0(\omega_0)$ is the initial wave energy density at any frequency ω_0 . The initial energy density and the initial wave flux evaluated at ω are related by (Jatenco-Pereira & Opher 1989):

$$\phi_{A_0}(\omega) = \epsilon_0(\omega) v_{A_0} \left(1 + \frac{3}{2} M_0 \right). \quad (22)$$

In our model, we adopt an initial wave flux as estimated by Hartmann & MacGregor (1980):

$$\phi_{A_0} = \int_{\omega_{\min}}^{\omega_{\max}} \phi_{A_0}(\omega) d\omega \simeq 10^6 \text{ erg cm}^{-2} \text{ s}^{-1}. \quad (23)$$

From equations (14), (15), and (20) we can write the temperature variation as:

$$\frac{dT}{dr} = \frac{2T}{3r} \left[\frac{r(Q - P_R)}{\rho u (k_B T/m)} - \left(Z + \frac{r}{u} \frac{du}{dr} \right) \right] \quad (24)$$

and the velocity variation as:

$$\begin{aligned} & \frac{1}{u} \frac{du}{dr} \left[u^2 - \frac{5k_B T}{3m} - \frac{\epsilon}{4\rho} \left(\frac{1+3M}{1+M} \right) \right] = \\ & = \frac{Z}{r} \left[-\frac{2r(Q - P_R)}{3Z\rho u} + \frac{\epsilon}{4\rho} \left(\frac{1+3M}{1+M} \right) \right] + \\ & + \frac{5k_B T}{3m} + \frac{r}{2Z\rho} \int_{\omega_{\min}}^{\omega_{\max}} \frac{\epsilon(\omega)}{L(\omega)} d\omega - \frac{v_e^2}{Z}, \end{aligned} \quad (25)$$

where we define Z as:

$$Z \equiv \begin{cases} S & \text{if } r \leq r_t \\ 2 & \text{if } r > r_t. \end{cases}$$

Hence, in order to obtain the velocity and the temperature profiles of the wind, we then solve equations (13), (24), and (25), simultaneously, for the wind of a typical K5 supergiant star.

2.4. Radiation Pressure

As in Paper I, we include the radiation pressure into the wind equation using an effective escape velocity:

$$\frac{1}{2} v_e^2 = \frac{GM_\star}{r} (1 - \Gamma), \quad (26)$$

where Γ is the ratio between the force per unit volume exerted on n_d grains of radius a situated at a distance r from a star of luminosity L_\star [$n_d \pi a^2 Q_d L_\star / (4\pi c r^2)$] and the gravitational force per unit volume ($\rho GM_\star / r^2$):

$$\Gamma = \frac{n_d \pi a^2 Q_d L_\star}{\rho 4\pi c GM_\star}. \quad (27)$$

Here Q_d is the mean extinction efficiency factor of the grain. In order to analyze how effective the radiation pressure is on the grains, we make a simple estimate. For silicate grains with $a \simeq 5 \times 10^{-6}$ cm in the atmosphere of a star with an effective temperature of 3500 K, we have $Q_d \sim 10^{-3}$ (Gilman 1974). We can write: $n_d/\rho = \rho_d/(\rho m_d) = (\mathcal{R}_{gd} m_d)^{-1}$. Then, if we assume that $\mathcal{R}_{gd} \simeq 200$, we obtain $\Gamma \simeq 0.03$; that is, the radiation pressure modifies the square of the escape velocity by only $\sim 3\%$. This is not a significant modification.

In Paper I, larger grains were considered. As Q_d is more important for large grains, it was shown in Paper I that radiation pressure leads to significant higher terminal velocities, although it can not initiate the wind. It is observed that the wind forms before the grain formation point (Carpenter et al. 1995), which indicates that another mechanism is taking place in order to drive the wind.

In the present model, we observe only a negligible difference in the terminal velocity if we consider the radiation pressure or not. This happens because we are adopting the radius distribution given by equation (1), which causes our model to have many more small grains than large ones.

3. RESULTS AND DISCUSSION

For the solution of the set of equations (13), (24), and (25), we adopted the set of initial conditions presented in Table 1 for the wind of a typical K5 supergiant star. We solve these equations until $r = 300 r_0$, at which point the wind has already reached its terminal velocity. Some parameters adopted here, such as the stellar mass, the stellar radius, the initial density, and the initial magnetic field, all have of the same values as the ones adopted by Hartmann & MacGregor (1980) for their model 6. The parameters calculated for the dust grains are shown in Table 2.

The momentum equation (eq. [25]) of the wind has a critical point when both the numerator and denominator go to zero. The requirement that the wind velocity should increase through the critical point determines the initial velocity at the base of the wind, i.e., $du(r = r_0)/dr \geq 0$. Hence, to find the critical solution for a given set of initial conditions, we iterate the initial velocity u_0 until the solution passes through the critical point. Together with the initial density, the initial velocity determines the mass-loss rate.

To simplify the problem, we calculate ω_{\min} and ω_{\max} at $r = r_0$ and assume that these parameters are constant throughout the wind. The grains charges are evaluated according to equation (5). Our results are shown in Figures 2 and 3, where we plot the velocity and the temperature profiles that we obtained. In order to have a better view of what is happening near the stellar surface, we plot the profiles until $r = 30 r_0$.

The results of the present model compares favorably with observations. We expect the terminal velocity to be lower than the surface escape velocity. From observations, we expect $u_\infty \sim v_{e0}/2$. Our model provides $u_\infty \simeq 57 \text{ km s}^{-1}$ and $\dot{M} \simeq 2.5 \times 10^{-7} \text{ M}_\odot \text{ yr}^{-1}$. In Figure 2, we can see that the wind is accelerated near the surface, even before the grain formation point ($\sim 2 r_0$).

As we know from solar corona observations, we expect a rise in the wind temperature near the stellar surface. From Figure 3, it can be seen that the rise in the temperature occurs very abruptly near the wind base. This heating is explained by the mechanical dissipation of Alfvén waves. At larger distances ($r \gtrsim 30 r_0$), the flow expands adiabatically, hence, in the absence of strong heating, the temperature tends to fall monotonically with the adiabatic exponent $4/3$.

In order to analyze the wave dissipation, we plot in Figure 4 the energy density of the waves at different distances from the star. At $r = r_0$, we have a power-law spectrum (eq. [21]). As we get farther from the wind base, the energy density decreases due to the flow expansion and wave damping. In Figure 4, we note that this decline is larger for larger wave frequencies, indicating a more efficient damping for waves with higher frequencies. This is due to the fact that we have a larger number of small-radius grains (see eq. [1]). As the smaller grains have larger cyclotron frequencies, they interact with the higher frequency waves, causing a larger damping at this spectral range.

Jatenco-Pereira & Opher (1989) studied the mass loss in late-type supergiants using three different damping mechanisms: nonlinear damping, resonant surface damping, and turbulent damping. They showed that these damping mechanisms have similar behaviors in the wind. In Figure 5, we compare the wave flux ϕ_A calculated by Jatenco-Pereira & Opher (1989), damped by the resonant surface damping, and the frequency-integrated flux calculated by the present model; that is, damped by the dust-cyclotron mechanism. It can be seen that the damping of the waves by the dust-cyclotron mechanism is not as efficient as any of the others mechanisms studied by Jatenco-Pereira & Opher (1989): at $\sim 4 r_0$ the wave flux has dropped by more than a factor of 10^2 in the model of Jatenco-Pereira & Opher (1989). Also, the dust-cyclotron damping mechanism is not as strong as the exponential decay that was simulated in Paper I. Nevertheless, our model can reproduce observational data such as the mass loss rate and the terminal velocity for the wind of a typical K5 supergiant star.

4. CONCLUSIONS

In this work, we consider an outward-directed flux of damped Alfvén waves as an acceleration mechanism for driving late-type stellar winds. As these winds present great amounts of dust particles and as the dust can modify the wave modes, we study here how the dust can affect the propagation of Alfvén waves, taking into account a specific damping mechanism, dust-cyclotron damping, which can be understood as follows. A charged grain immersed in a magnetized plasma possesses a cyclotron frequency associated with it. If Alfvén waves are present in this plasma, their propagation near the dust-cyclotron frequency can be affected.

As different grain sizes carry different charges, there will be a cyclotron frequency associated with each grain size. In this sense, a dust size distribution has several dust-cyclotron frequencies, which will affect a broad band of Alfvén wave frequencies.

We also calculated the radiation pressure exerted on grains. We included this force as another acceleration mechanism of the wind. As we adopted great amounts of small grains, we observed only a negligible difference in the wind velocity profile from what we would have obtained if we did not consider radiation pressure.

Our model also assumes a diverging geometry for the magnetic field lines. This assumption is based on the observations of coronal holes in the Sun, which present a superradial expansion of magnetic field lines. Thus, the mass, momentum, and energy equations are obtained and then solved in a self-consistent approach.

Our results of wind velocity and temperature profiles for a typical K5 supergiant star shows compatibility with observations. We also show that, considering the presence of charged dust particles, the wave flux is less damped due to dust-cyclotron damping than it would be if we considered some other damping mechanisms studied in the literature, such as nonlinear damping, resonant surface damping, and turbulent damping.

The authors would like to thank the Brazilian agencies FAPESP (under grant 02/10846-0) and CNPq (under grant 304523/90-9) for financial support.

REFERENCES

- Ayres, T. R., Brown, A., & Harper, G. M 2003, *ApJ*, 598, 610
- Banerjee, D., Teriaca, L., Doyle, J. G., Wilhelm, K. 1998, *A&A*, 339, 208
- Blackman, E. G., Frank, A., Markiel, J. A., Thomas, J. H. & Van Horn, H. M. 2001, *Nature*, 409, 485
- Carpenter, K. G., Robinson, R. D., & Judge, P. G. 1995, *ApJ*, 444, 424
- Cassinelli, J. P. 1979, *ARA&A*, 17, 275
- Cramer, N.: 2001, in "The Physics of Alfvén Waves", Wiley, Berlin
- Cramer, N., Verheest, F., & Vladimirov, S. 2002, *Phys. Plasmas*, 9, 4845
- Cranmer, S. R., & van Ballegooijen, A. A. 2005, *ApJS*, 156, 265

- Dominik, C., Sedlmayr, E., & Gail, H. P. 1989, *A&A*, 223, 227
- Dorch, S. B. F. 2004, *A&A*, 423, 1101
- Elitzur, M., & Ivezić, Z. 2001, *MNRAS*, 327, 403
- Esser, R., Lie-Svendsen, Ø., Janse, Å.M., & Killie, M. A. 2005, *ApJ*, 629, 61
- Falceta-Gonçalves, D. & Jatenco-Pereira, V. 2002, *ApJ*, 576, 976, Paper I
- Falceta-Gonçalves, D., de Juli, M. C., & Jatenco-Pereira, V. 2003, *ApJ*, 597, 970
- Gilman, R. C. 1974, *ApJS*, 28, 397
- Goertz, C. 1989, *Rev. Geophys.*, 27, 271
- Hartmann, L., & MacGregor, K. B. 1980, *ApJ*, 242, 260
- Hartmann, L., Edwards, S., & Avrett, E. 1982, *ApJ*, 261, 279
- Heras, A. M., & Hony, S. 2005, *A&A*, 439, 171
- Höfner, S., Gautschy-Loidl, R., Aringer, B., & Jørgensen, U. G. 2003, *A&A*, 399, 589
- Hollweg, J. V. 1973, *ApJ*, 181, 547
- Holzer, T. E., Flå , T., & Leer, E. 1983, *ApJ*, 275, 808
- Jatenco-Pereira, V., & Opher, R. 1989 *A&A*, 209, 327
- Knapp, G.R. 1985, *ApJ*, 293, 273
- Kuin, N. P. M., & Hearn, A. G. 1982, *A&A*, 114, 303
- Lamers, H. J. G. L. M., & Cassinelli, J. P. 1999, *Introduction to stellar winds* (New York: Cambridge University Press)
- Liberatore, S., Lafon, J.-P. J., & Berruyer, N. 2001, *A&A*, 377, 522
- Lie-Svendsen, O., Hansteen, V. H., & Leer, E. 2002, *ApJ*, 566, 562
- Mathis, J., Rumpl, W., & Nordsiek, K. 1977, *ApJ*, 217, 425
- Mendis, D., & Rosenberg, M. 1992, *IEEE Trans. Plasma. Sci.*, 20, 929
- Mendis, D., & Rosenberg, M. 1994, *ARA&A*, 32, 419

- Parker, E. (1965), *Space Science Reviews*, 4, 666
- Peter, H., & Judge, P. G. 1999, *ApJ*, 522, 1148
- Pillip, W., Morfill, G., Hartquist, T., & Havnes, O. 1987, *ApJ*, 314, 341
- Rodgers, B., & Glassgold, A. E. 1991, *ApJ*, 382, 606
- Rosenthal, C. S., Bogdan, T. J., Carlsson, M., Dorch, S. B. F., Hansteen, V., McIntosh, S. W., McMurry, A., Nordlund, Å, & Stein, R. F. 2002, *ApJ*, 564, 508
- Sandin, C., Höfner, S. 2003, *A&A*, 404, 789
- Schmutzler, T., & Tscharnuter, W. M. 1993, *A&A*, 273, 318
- Shukla, P. 1992, *Phys. Scr.*, 45, 504
- Soker, N., & Zoabi, E. 2002, *MNRAS*, 329, 204
- Suzuki, T. K., & Inutsuka, S. 2005, *ApJ*, 632, 52
- Tu, C. Y., Marsch, E., & Thieme, K. M. 1989, *J. Geophys. Res.*, 94, 11739
- Tu, C.-Y., Zhou, C., Marsch, E., Xia, L.-D., Zhao, L., Wang, J.-X., Wilhelm, K. 2005, *Science*, 308, 519
- Vladimirov, S. V. 1997, *Ap&SS*, 256, 85
- Vlemmings, W. H. T., Diamond, P. J., & van Langevelde, H. J. 2002, *A&A*, 394, 589
- Wardle, M., & Ng, C. 1999, *MNRAS*, 303, 239
- Woitke, P., & Niccolini, G. 2005, *A&A*, 433, 1101

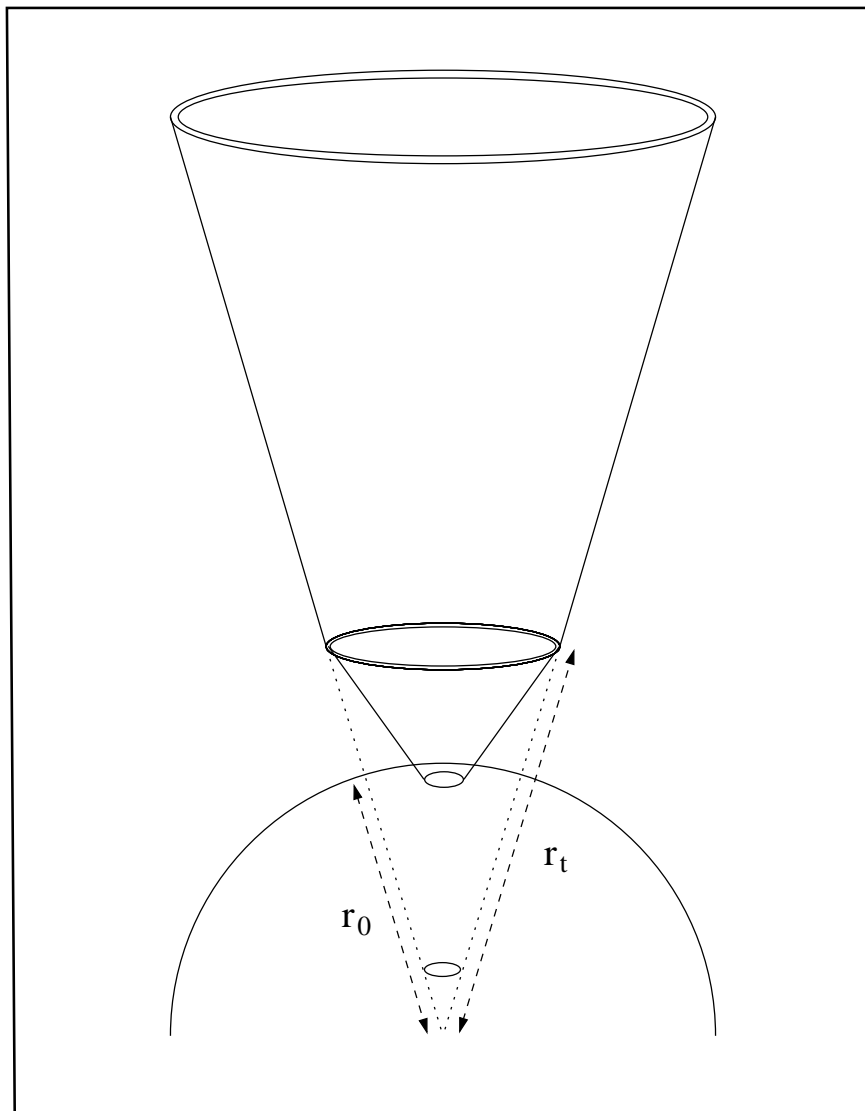


Fig. 1.— Geometry used in order to reproduce coronal holes (not to scale).

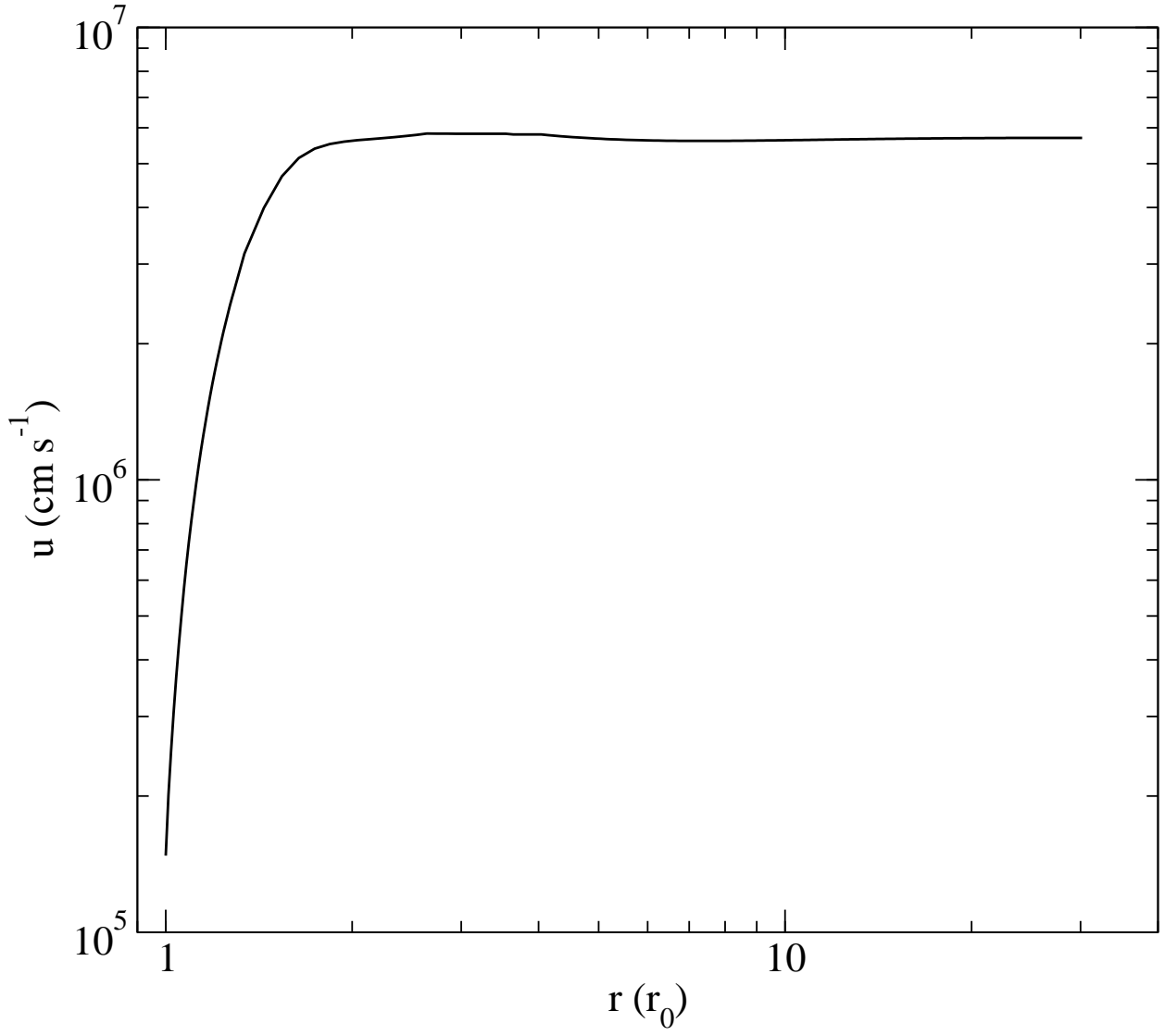


Fig. 2.— Wind velocity profile obtained for a typical K5 supergiant star.

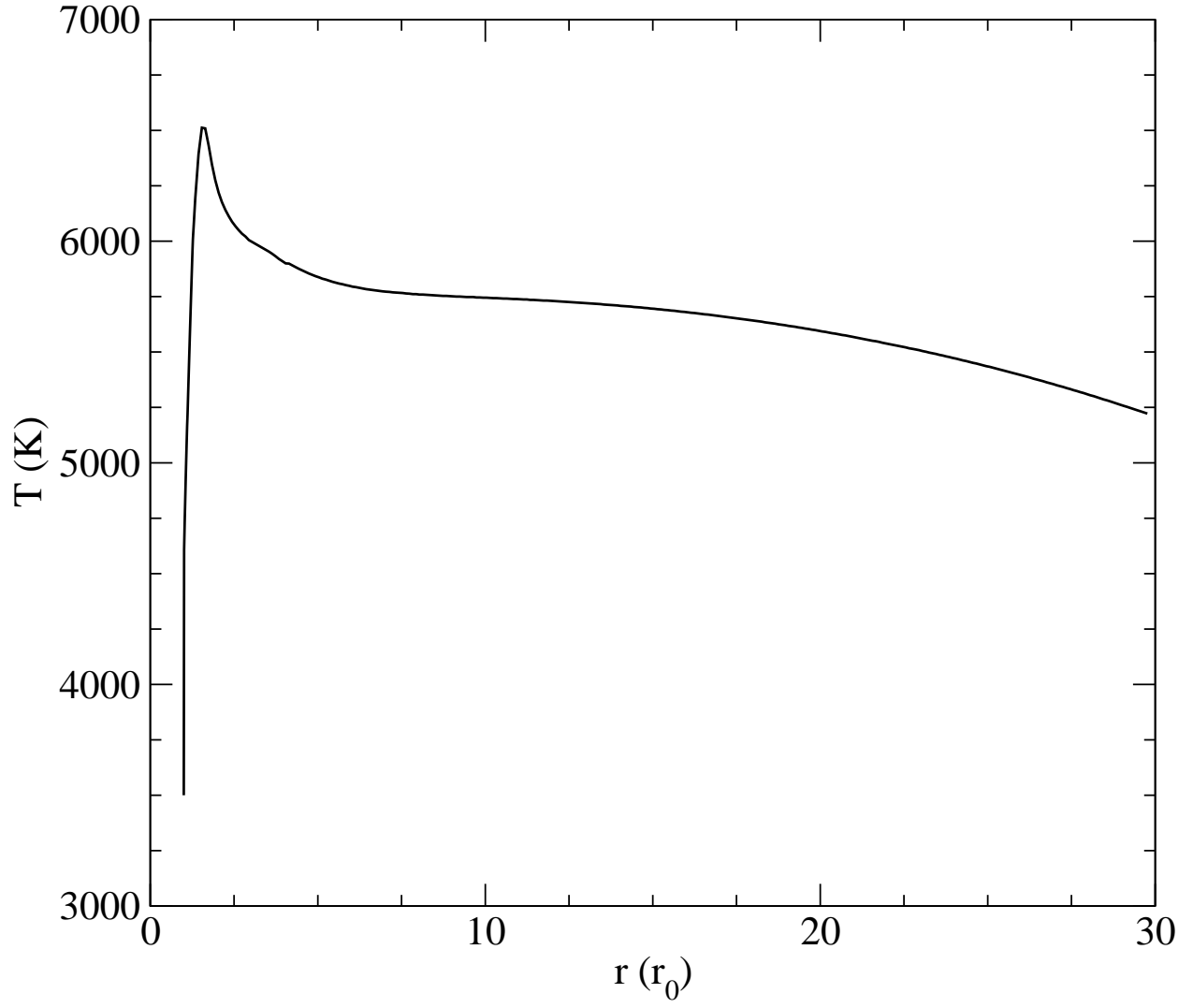


Fig. 3.— Wind temperature profile obtained for a typical K5 supergiant star.

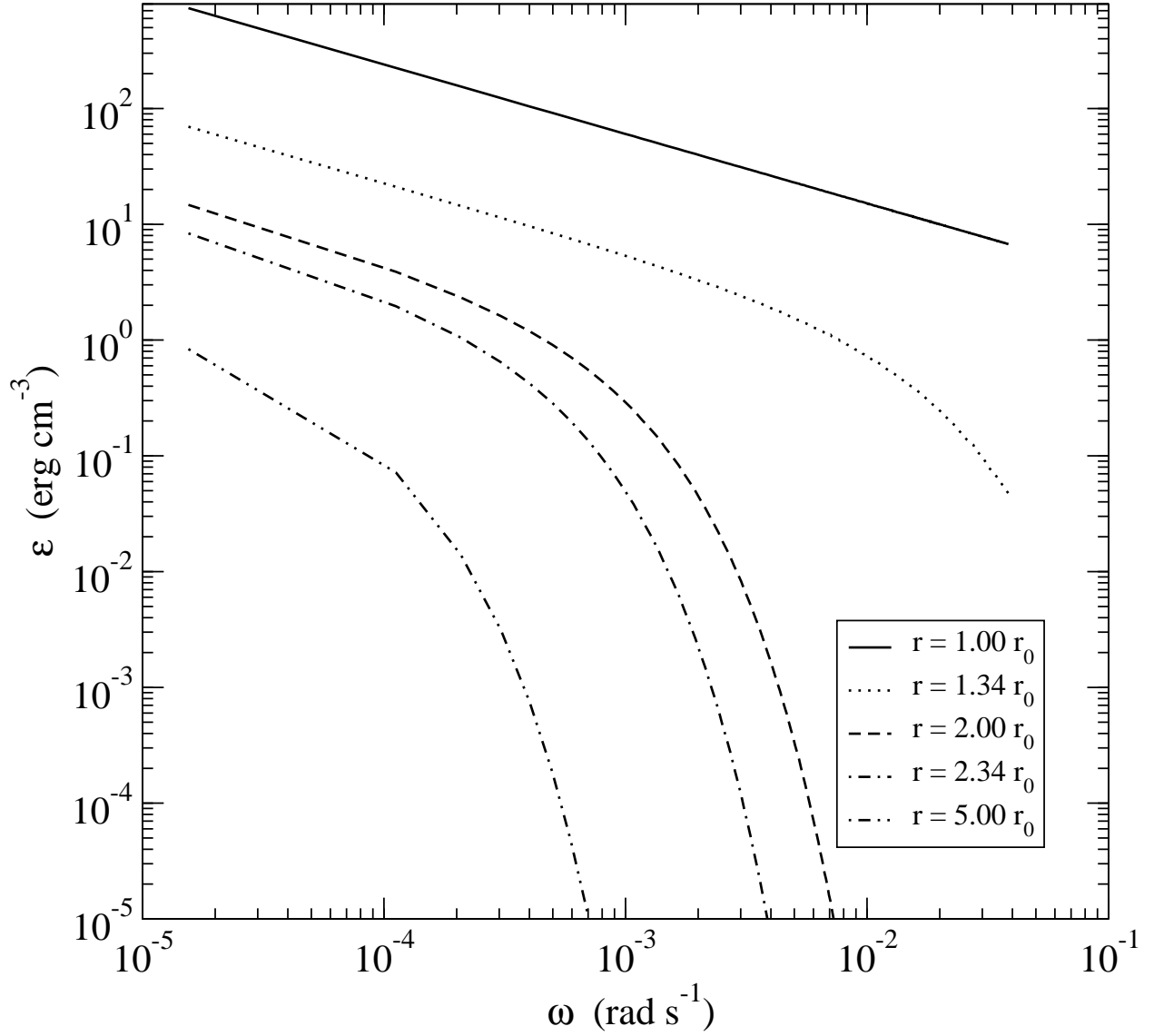


Fig. 4.— Energy density of Alfvén waves at different positions: at $1 r_0$ (solid curve), at $1.34 r_0$ (dotted curve), at $2 r_0$ (dashed curve), at $2.34 r_0$ (dash-dotted curve), and at $5 r_0$ (dash-double-dotted curve).

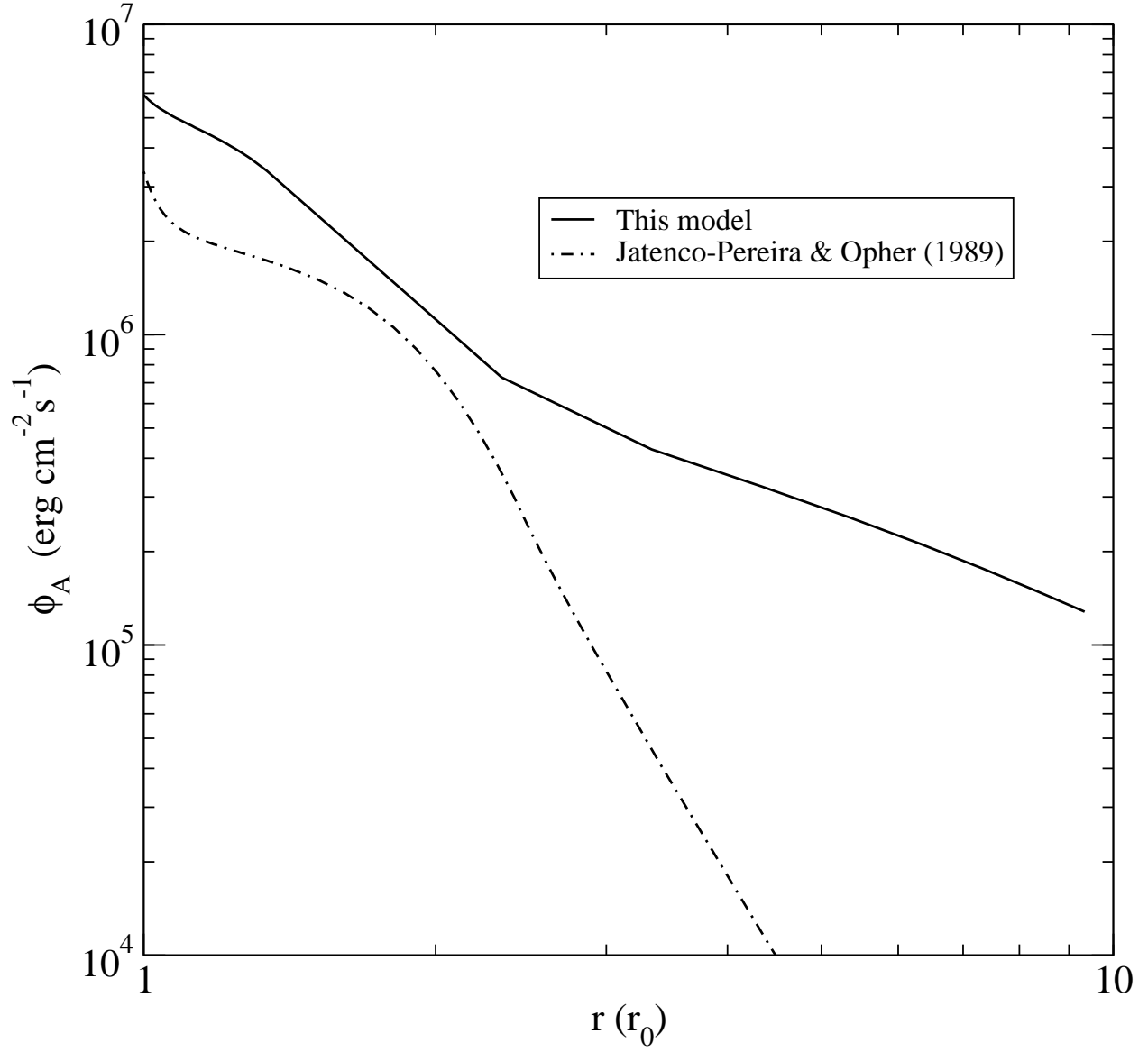


Fig. 5.— Comparison between Alfvén waves fluxes for this model (solid curve) and for the model of Jatenco-Pereira & Opher (1989) (dash-dotted curve).

Table 1: Initial parameters adopted for the wind of a typical K5 supergiant star.

Parameter	Value	Unity
r_0	400	R_\odot
M_\star	16	M_\odot
ϕ_{A_0}	5.5×10^6	$\text{erg cm}^{-2} \text{s}^{-1}$
ρ_0	1.07×10^{-13}	g cm^{-3}
u_0	1.5×10^5	cm s^{-1}
B_0	10	G
T_0	3500	K
S	4.0	-
r_t	3.16	r_0

Table 2: Maximum and minimum calculated initial dust charges and cyclotron frequencies related to the minimum grain radius ($a_{\min} = 5.0 \times 10^{-7}$ cm) and the maximum grains radius ($a_{\max} = 2.5 \times 10^{-5}$ cm).

Parameter	Value	Unity
q_{\min}	2.6	e
q_{\max}	131.2	e
ω_{\min}	9.7×10^{-5}	rad s^{-1}
ω_{\max}	2.4×10^{-1}	rad s^{-1}